32nd Annual International Conference of the IEEE EMBS
Buenos Aires, Argentina, August 31 - September 4, 2010

A Biomechanical Model for the Development of Myoelectric Hand Prosthesis Control Systems

Bart Peerdeman*, Daphne Boere†, Laura Kallenberg†, Stefano Stramigioli*, and Sarthak Misra*

Abstract— **Advanced myoelectric hand prostheses aim to reproduce as much of the human hand's functionality as possible. Development of the control system of such a prosthesis is strongly connected to its mechanical design; the control system requires accurate information on the prosthesis' structure and the surrounding environment, which can make development difficult without a finalized mechanical prototype. This paper presents a new framework for the development of electromyographic hand control systems, consisting of a prosthesis model based on the biomechanical structure of the human hand. The model's dynamic structure uses an ellipsoidal representation of the phalanges. Other features include underactuation in the fingers and thumb modeled with bond graphs, and a viscoelastic contact model. The model's functions are demonstrated by the execution of lateral and tripod grasps, and evaluated with regard to joint dynamics and applied forces. Finally, future work is suggested with which this model can be used in mechanical design and patient training as well.**

I. Introduction

The loss of an upper limb is a life-altering event. It involves not only the loss of the appendage itself, but also the disruption of the intricate systems that plan and execute its motions. Through advanced prostheses, modern technology is able to replicate a small part of the human hand's functionality; however, in performing normal daily activities the patient's ability to control a prosthesis' limited functions is as essential as the functions themselves. To this end, most current prostheses combine a sensing system to ascertain the user's intended motion with a control system to execute that motion with the correct speed and force. The development of such a control system requires knowledge of the exact structure of the prosthesis, as well as information about the environment obtained through sensors. A model of the prosthesis can be used to support control system development when a physical prototype is not available. Further, any changes to the mechanical design can be accommodated in the model and the necessary sensor information can be directly extracted from the state of the model.

Humanoid hand models have been developed by other groups for various purposes. Many are realistic reproductions of the human hand, for medical or industrial applications [1], [2], [3]. Other models are used for the generation of realistic computer graphics [4]. In robotics, GraspIt! [5] is a software package for simulation and grasp planning of a wide variety of robotic hands, though it does not support user level control. For prosthetics, besides virtual setups to aid in user training [6], a good example of a kinematic model can be found in Dragulescu and Ungureanu [7]. However, that model's number of degrees of freedom (DOFs) was reduced to fifteen from an initial twenty-three, and it lacks physical contact modeling.

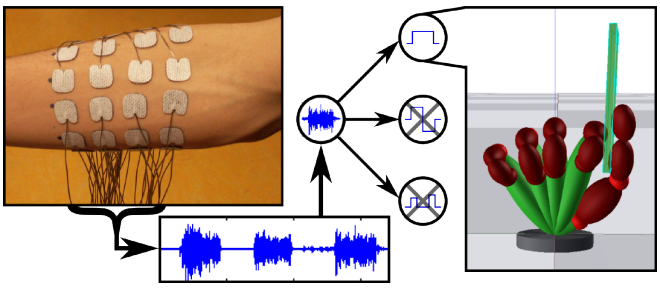

Fig. 1. **Diagram representing signal processing from electromyographic sensing to control:** Myoelectric signals are acquired and classified, leading to control signals for grasp selection and execution. These signals are then sent to the model, where they control the motions of a virtual representation of a prosthetic hand.

In this paper, a model based on the human hand's biomechanical structure is demonstrated. This model serves as a testbed for the development of control systems based on electromyographic (EMG) input, which is the current standard in the non-invasive control of electrically powered prostheses. Myoelectric signals are the electrical expression of the neuromuscular activation generated by skeletal muscles [8]; they are rich in information regarding the user's intent and can therefore serve as an effective control input. The information derived from these signals is transferred to the control system (Figure 1), which determines and executes the specific motions of which the intended movement consists. The parameters of this model are based on analysis of human hand dimensions [1], [9] and inertial properties [10]. The underactuated joints of the fingers and thumb are connected through a system of bond graphs, which model the distribution of motor torque across the joints. A contact model based on [11] is implemented, using an ellipsoidal approximation of the phalanges.

The sensing and control systems that provide input to the model are detailed in Section II. Section III contains details on the model's high-level structure, and the parameters and equations that make up the model. In Section IV, the results of several simulated grasps are discussed. We conclude with Section V and provide directions for future work.

* Control Engineering Group, University of Twente, The Netherlands.
† Roessingh Research and Development, The Netherlands.
This research is funded by the Dutch Ministry of Economic Affairs and the Province of Overijssel, within the Pieken in de Delta (PIDON) initiative.
All authors are affiliated with MIRA - Institute for Biomedical Technology and Technical Medicine, University of Twente.

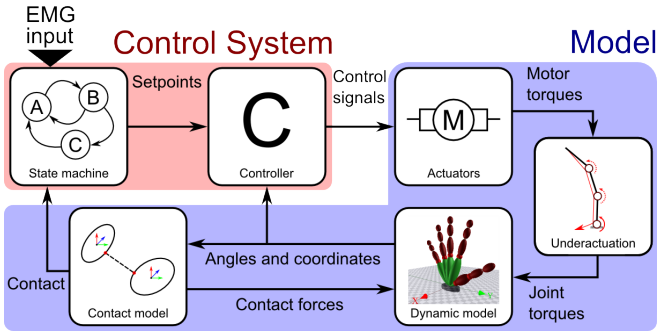

Fig. 2. Block diagram illustrating the flow of information through the control system and model.

II. EMG Input and Control System

The block diagram describing the interactions between the different parts of the control system and model can be seen in Figure 2. The input of the control system is generated by an EMG sensing system. EMG sensing uses surface electrodes to detect the myoelectric potential generated when a muscle contracts. However, the potential arriving at the electrodes is very small in comparison to other detected signals, e.g. cardiac-related noise, environment noise and motion artefacts. Therefore, amplification and a filtering method must be applied to reduce these noise signals [12], [13]. In most current EMG systems, the signal data is then segmented into small intervals of which features (i.e. characteristic parameters related to user intent) are extracted. Several parameters in the time, frequency, and time-frequency domains can be used as features, such as the root mean square, mean absolute value, mean frequency, and wavelet transform coefficients.

Detection of a certain number of intended actions requires the same number of unique muscle activity patterns. Each pattern is described by a specific set of features that are entered into a classifier, which determines the movement intended by the user [13], [14], [15]. Examples of frequently used classifiers in literature are linear discriminant analysis [16] and artificial neural networks [17]. In this study, the results of the classification process are gathered into a sensing vector, serving as the EMG input in Figure 2. This vector is made up of elements indicating the intended grasp type [18], direction and force of opening/closing of the hand, and the direction and speed of wrist movement. Implementation of wrist control is straightforward, and will be done in a future version of the model.

A grasp type determines two things: the starting pose of the hand, and the relative timing between flexion of the individual fingers and thumb. When a certain grasp type is detected by EMG sensing, the control system will automatically move the relevant joints to their starting angles. This process is called preshaping. Once the grasp is preshaped, hand opening/closing and wrist movement signals control the execution of the grasp. The interaction between high-level EMG user input and low-level prosthesis control signals can be described by a set of state machines. Through the control signals contained in the sensing vector, the user can change the state of the control system, which determines the

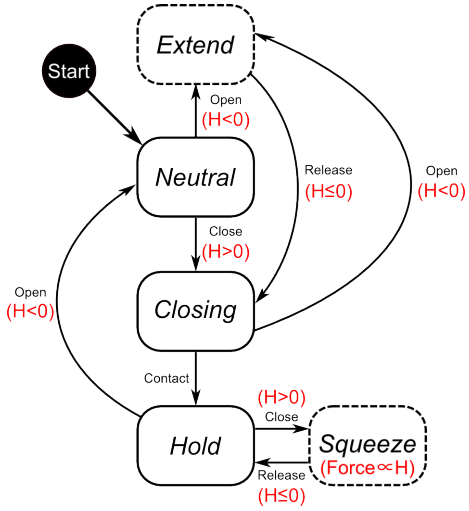

Fig. 3. **Hand opening/closing state machine:** H is the part of the sensing vector related to hand opening/closing, with negative values for opening and positive values for closing. The absolute value of the signal determines the force applied in the *Squeeze* state. States with a dashed border are exited automatically when no signal is received.

automated low-level behavior of the prosthesis. The state machine describing the hand opening/closing behavior is shown in Figure 3.

Similar to the Southampton Adaptive Manipulation Scheme [19], this system allows the user to switch between basic grasping states using a single control signal (hand opening/closing, or H). Starting from the *Neutral* state where preshaping takes place, the grasp can be closed using a single close signal (H>0). The *Closing* of the grasp continues automatically at fixed speed until interrupted by an open signal (H<0) or contact is detected by the model. In the *Hold* state, the prosthesis will automatically apply sufficient force to counteract slipping of the held object. The *Extend* state enables grasping of larger objects, and the *Squeeze* state gives the user direct control over the force applied to a held object. This system is arranged to allow opening and closing of a grasp with a minimal number of commands for ease of use. Based on the state of the control system and feedback from the model, desired torque values are sent to the model to control the joint angles and applied forces.

III. Model Structure

When the model receives the desired actuator torques from the control system, the individual joint torques are determined by an underactuation model. It represents the tendon-and-pulley mechanisms that are present in many modern hand prostheses [20], [21], [22] to reduce the number of actuators required. This type of underactuation also provides a natural and effective grasping motion; when one of the phalanges of a finger encounters an object, the other phalanges automatically continue wrapping around it. The finger underactuation is modeled using bond graphs [23]. Bond graphs are an inherently energy conserving and domain independent way of modeling dynamic systems. Additionally, the equations describing the behavior of the system can be algorithmically derived from the graph itself.

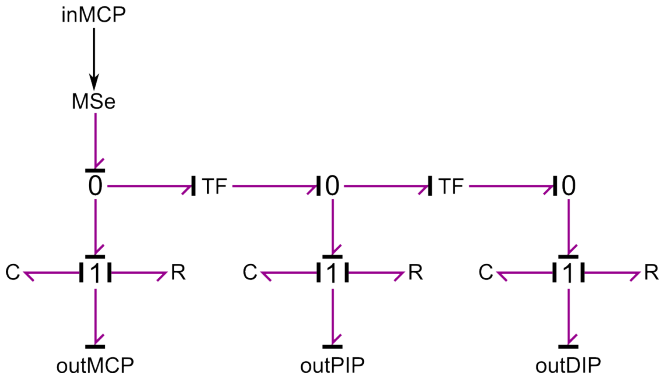

Fig. 4. **Bond graph of index finger underactuation:** The actuator is represented by a modulated effort source (MSe) element, providing torque which is distributed across the joints through junction (0, 1) and transformer (TF) elements. The capacitive (C) and resistive (R) elements represent the individual joints' stiffness and friction, respectively.

As an example, the bond graph representing underactuation of the index finger is shown in Figure 4; similar graphs are implemented on the other fingers and thumb. This system distributes actuator torque across the joints based on their relative stiffnesses and friction. The stiffnesses of the joints are based on [24], [25], and the friction parameters were determined by own experimentation. When all joint torques have been calculated, they are entered into the dynamic model, which represents the kinematic structure of the hand.

The dimensions, joint locations, and other parameters of the dynamic model are based on those of the human hand, the bone and joint structure of which can be seen in Figure 5. The fingers' interphalangeal (IP) joints are functionally equivalent to one-DOF flexion/extension joints. The metacarpophalangeal (MCP) joints at the base of the fingers have an additional abduction/adduction DOF. The thumb contains five DOFs: one (flexion/extension) in its IP joint, and two in both its MCP and carpometacarpal (CMC) joints [26]. In reality, the latter two joints have a complicated surface geometry, resulting in joint axes that are neither completely perpendicular nor coincident. In this model these are approximated by two-DOF flexion/extension and abduction/adduction joints. The individual joint ranges of motion are implemented as described in [27], [28].

In [9], the average dimensions of the human hand were examined in detail. A linear relation between hand segment sizes and hand breadth/length was determined, the results of which can be found in Table I. These dimensions can be used to approximate the phalanges by ellipsoid bodies [9]. Although this approximation does have significant deviations near the joints, this causes no problems during normal grasping; the parts of the phalanges that contact an object lie near the middle of the ellipsoids or at the tips of the fingers.

The average inertial parameters of the human hand were described in [10]. In this model, the individual phalanges' inertial parameters are approximated using the inertia tensor equations for a homogeneous ellipsoid with radii a, b, c as in Table I, and mass m (all other components of the inertia

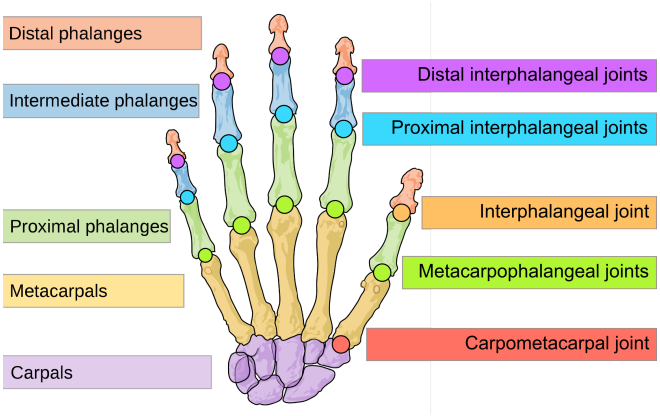

Fig. 5. **Bone and joint structure of the human hand:** Bone names are listed on the left, while joint names are on the right (This figure is an edited version of the original presented in [29]).

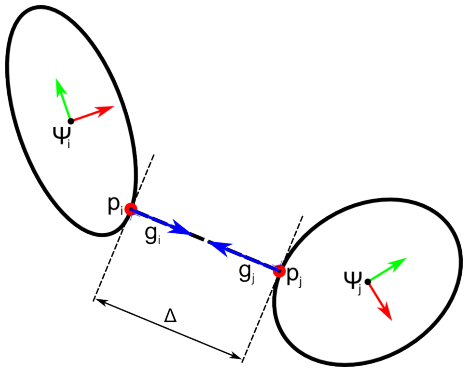

Fig. 6. Closest point calculation of two ellipses (i, j) with minimal distance Δ. Note that the perpendicular vectors g_* are directly opposed to one another at the contact points p_*.

tensor $\mathcal{I}$ are 0):

$$\mathcal{I}_{xx} = 0.2m(b^2 + c^2).$$
$$\mathcal{I}_{yy} = 0.2m(a^2 + c^2).$$
$$\mathcal{I}_{zz} = 0.2m(a^2 + b^2).$$

With the implementation of the dynamic model, the system is able to determine the effect of internally applied forces and torques. To complete the model, interaction forces with the environment and the hand itself have to be computed as well, using a contact model. A contact model needs to determine when and where two bodies intersect one another, and calculate the forces that need to be applied to the contacting bodies.

The points of least distance between an ellipsoid of the dynamic model and a plane (with which various test objects can be constructed) can be determined analytically [30]. Between two of the model's ellipsoids, this solution no longer applies and another method is required. In [11] such a method is described; a two-dimensional example can be seen in Figure 6. Take two three-dimensional ellipsoids (i, j) with coordinate frames Ψ_* and points of least distance p_* , where $*$ is i or j. At these points, separated by a distance Δ, the normal vectors g_* of the ellipsoids are directly opposed to one another. Taking P_i^j as the coordinates of

TABLE I

AVERAGE RADII OF MODEL PHALANGE ELLIPSOIDS (a, b, c), RELATIVE TO TOTAL HAND BREADTH (a, b) AND HAND LENGTH (c) [1], [9].

	Thumb	Index	Middle	Ring	Little
Carpal	(0.10,0.10,0.06)	-	-	-	-
Metacarpal	(0.07,0.08,0.13)	(0.10,0.12,0.23)	(0.09,0.13,0.22)	(0.09,0.14,0.21)	(0.08,0.13,0.21)
Proximal	(0.05,0.05,0.10)	(0.05,0.05,0.12)	(0.06,0.05,0.13)	(0.06,0.05,0.12)	(0.05,0.05,0.10)
Intermediate	-	(0.05,0.05,0.07)	(0.05,0.05,0.09)	(0.04,0.05,0.08)	(0.04,0.04,0.06)
Distal	(0.05,0.06,0.08)	(0.04,0.05,0.05)	(0.04,0.05,0.05)	(0.04,0.05,0.05)	(0.04,0.04,0.05)

point p_i in frame Ψ_j and H_j^i as the homogeneous coordinate transformation between coordinate frames j and i, Δ can be defined as the following inner product $(\langle , \rangle)$ [11]:

$$\Delta = \left\langle g_i, (H_j^i P_j^j - P_i^i) \right\rangle = \left\langle g_j, (H_i^j P_i^i - P_j^j) \right\rangle$$

Note that this distance will become negative as the bodies pass through one another, which allows contact to be defined as a zero crossing. The relationship between the coordinates P_i^i and P_j^j can be written as a function of g_j, Δ, and H_j^i as follows:

$$P_i^i - \Delta H_j^i g_j = H_j^i P_j^j$$

By then taking the time derivative of both these equations, with $\tilde{T}_j^{i,i}$ as a skew-symmetric matrix containing the translational and rotational velocities of frame j with respect to frame i expressed in frame i, the time derivative of these coordinates can be calculated by [11]:

$$\left(\dot{g}_i + H_j^i \dot{g}_j H_i^j \left(I + \Delta \dot{g}_i\right)\right) \dot{P}_i^i = \tilde{T}_j^{i,i} g_i + H_j^i \dot{g}_j \left(\dot{\Delta} g_j - \tilde{T}_i^{j,j} P_j^j\right)$$

The equations provided above allow analytical calculation of the movement of the two points of least distance, given the initial conditions which can be found through numerical iteration. When the distance between these points crosses below zero, contact has been established. The resulting forces applied to the colliding bodies are modeled viscoelastically, by combination of linear elastic and damping elements. With all model subsystems in place, the model can be tested, using data from the EMG sensing vector to directly control the grasping of a simple object.

IV. MODEL APPLICATIONS AND RESULTS

A pair of basic grasp types are executed to test the model's performance: a lateral grasp and a tripod grasp. For both grasps, the control system will receive an EMG sensing vector containing a grasp selection signal, followed by a hand close signal. The preshaping of the lateral grasp consists of minimal thumb opposition and full flexion of all fingers; preshaping of the tripod grasp requires the full flexion of the little and ring fingers, abduction of the index and middle fingers, and the thumb to be brought in opposition to the index and middle fingers.

The lateral grasp results are used to illustrate the model's response to the received EMG sensing vector, while the tripod grasp will show the functioning of the model's internal structure through a plot of the generated joint angles and

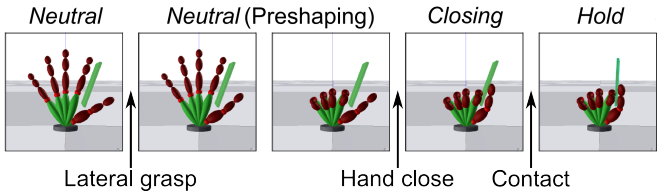

Fig. 7. Lateral grasp simulation results, indicating the control system's state (above) and received input from the EMG sensing vector and the environment (below). The control system's states are depicted in Figure 3.

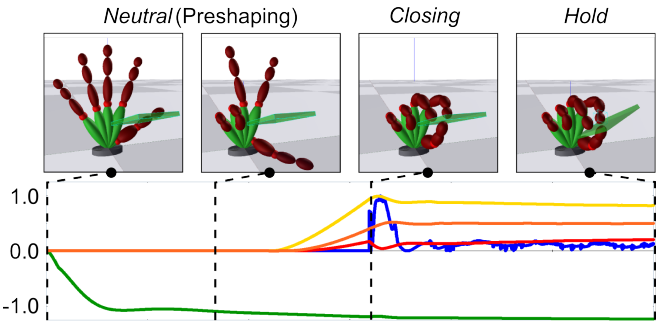

Fig. 8. Tripod grasp simulation results, showing the thumb's opposition angle (rad) in green, the individual thumb joint flexion angles (rad) in red (IP joint), orange (MCP joint) and yellow (CMC joint), and the normalized total contact force on the thumb in blue.

forces. The progress of the lateral grasp can be observed in Figure 7. First, the control system receives a grasp selection signal for the lateral grasp. This causes it to control the thumb to the proper opposition angle, and to fully flex all fingers (*Neutral*). The grasp is now fully preshaped, and when a hand close signal is received afterwards, the thumb is flexed at constant torque until a contact signal is received from the model (*Closing*). After contact, a continuous force is applied to keep the object in place (*Hold*).

The execution of the tripod grasp can be observed in Figure 8 along with several of the thumb's state variables, indicating the model's dynamic behavior. At the initial position, all joint angles are 0. When preshaping begins, the thumb opposition angle is controlled to the right position for the tripod grasp. After receiving the hand close signal, the underactuated structure of the thumb causes its joints to flex in a natural motion as motor torque is applied. When contact is made, the thumb's shape adapts to the object, which can be seen by the change in its joint angles as a consequence of the contact force. After the impact has been resolved, the joint angles stabilize. These figures demonstrate the successful operation of the model and control system.

V. Conclusions and Future Work

In this paper, a three-dimensional hand prosthesis model is described, based on the biomechanical structure of the human hand. The model's main purpose is as a testbed for the development of prosthesis control systems based on input from EMG sensing. The validity of the model was tested by executing two different grasp types on a simple object, demonstrating preshaping of the hand and subsequent flexion of the fingers and thumb. The correct operation of the finger underactuation, contact model and dynamic model have been demonstrated. This model can provide control systems with information including internal and external forces/torques, joint angles and velocities, and contact positions.

For future work on this model, the first point to be addressed is an extension of the dynamic model and control system to accommodate wrist motions. The addition of wrist rotation and flexion/extension would allow the model to exhibit the full functionality of modern hand prostheses.

In addition to control, the mechanical design of a hand prosthesis could be tested as well. Many recently developed prosthetic hands employ methods such as reduced thumb opposition DOFs [20], linked finger flexion [21] or passive joints [31]. This is done to reduce the number of required actuators, due to the prostheses' strict space and weight limitations. By establishing performance metrics based on grasping tests with this model, the relative effectiveness of models with mechanical simplifications could be evaluated.

Another future purpose of this system could be a combination of the model and an EMG-based control system into a virtual reality application for patient prosthesis training. For this to be useful, the user should be able to move the hand model in three dimensions as though it were connected to the forearm. An accelerometer mounted on the stump could be connected to the model to accomplish this. With the completion of these additions, this model could be used as a complete prosthesis design application. A prosthesis' control systems and mechanical design could then be tested and developed simultaneously, using input from patient trials to improve ease of use while optimizing functionality at the same time.

References

[1] B. Buchholz *et al.*, "Anthropometric data for describing the kinematics of the human hand," *Ergonomics*, vol. 35, no. 3, pp. 261–273, 1991.

[2] J. L. Sancho-Bru *et al.*, "A 3D biomechanical model of the hand for power grip," *Journal of Biomechanical Engineering*, vol. 125, no. 1, pp. 78–83, 2003.

[3] T. J. Armstrong *et al.*, "Development of a kinematic hand model for study and design of hose installation," in *Proceedings of the 2nd International Conference on Digital Human Modeling (ICDHM)*, San Diego, USA, pp. 85–94, July 2009.

[4] J. Kuch and T. Huang, "Human computer interaction via the human hand: a hand model," in *Proceedings of the Twenty-Eighth Asilomar Conference on Signals, Systems and Computers*, Pacific Grove, USA, pp. 1252–1256, October-November 1994.

[5] A. Miller and P. Allen, "Graspit!: A versatile simulator for robotic grasping," *IEEE Robotics and Automation Magazine*, vol. 11, pp. 110–122, Dec 2004.

[6] J. L. Pons *et al.*, "Virtual reality training and EMG control of the MANUS hand prosthesis," *Robotica*, vol. 23, no. 03, pp. 311–317, 2005.

[7] D. Dragulescu and L. Ungureanu, "The modeling process of a human hand prosthesis," in *Proceedings of the 4th International Symposium on Applied Computational Intelligence and Informatics (SACI)*, Timisoara, Romania, pp. 263–268, 2007.

[8] C. J. De Luca, *Encyclopedia of medical devices and instrumentation*. Boston, Massachusetts: John Wiley & Sons, Inc., 2006.

[9] B. Buchholz and T. J. Armstrong, "An ellipsoidal representation of human hand anthropometry," *Human Factors*, vol. 33, no. 4, pp. 429–441, 1991.

[10] R. F. Chandler *et al.*, "Investigation of inertial properties of the human body," 1975.

[11] V. Duindam and S. Stramigioli, "Modeling the kinematics and dynamics of compliant contact," in *Proceedings of the IEEE International Conference on Robotics and Automation (ICRA)*, Taipei, Taiwan, pp. 4029–4034, September 2003.

[12] e. a. Webster, J.G., *Medical instrumentation: application and design*. Hoboken, New Jersey: John Wiley & Sons Inc., 1998.

[13] M. Zecca *et al.*, "Control of multifunctional prosthetic hands by processing the electromyographic signal," in *Critical Reviews in Biomedical Engineering*, pp. 459–485, 2002.

[14] M. A. Oskoei and H. Hu, "Myoelectric control systems–a survey," *Biomedical Signal Processing and Control*, vol. 2, no. 4, pp. 275 – 294, 2007.

[15] B. Hudgins *et al.*, "A new strategy for multifunction myoelectric control," *Biomedical Engineering, IEEE Transactions on*, vol. 40, no. 1, pp. 82–94, 1993.

[16] K. Englehart *et al.*, "A wavelet-based continuous classification scheme for multifunction myoelectric control," *IEEE Transactions on Biomedical Engineering*, vol. 48, pp. 302–311, March 2001.

[17] F. C. P. Sebelius *et al.*, "Refined myoelectric control in below-elbow amputees using artificial neural networks and a data glove," *The Journal of Hand Surgery*, vol. 30, no. 4, pp. 780–789, 2005.

[18] M. R. Cutkosky, "On grasp choice, grasp models, and the design of hands for manufacturing tasks," *Robotics and Automation, IEEE Transactions on*, vol. 5, no. 3, pp. 269–279, 1989.

[19] P. Kyberd and P. H. Chappell, "The southampton hand: An intelligent myoelectric prosthesis," *Journal of Rehabilitation Research and Development*, vol. 31, no. 4, pp. 326–334, 1994.

[20] D. Yang *et al.*, "An anthropomorphic robot hand developed based on underactuated mechanism and controlled by EMG signals," *Journal of Bionic Engineering*, vol. 6, no. 3, pp. 255–263, 2009.

[21] C. Cipriani *et al.*, "Progress towards the development of the smarthand transradial prosthesis," in *Proceedings of the IEEE International Conference on Rehabilitation Robotics (ICORR)*, Kyoto, Japan, pp. 682–687, June 2009.

[22] S. A. Dalley *et al.*, "Design of a multifunctional anthropomorphic prosthetic hand with extrinsic actuation," *IEEE/ASME Transactions on Mechatronics*, vol. 14, no. 6, pp. 699–706, 2009.

[23] P. C. Breedveld, *Modeling and simulation of dynamic systems using bond graphs*. Oxford, UK: Eolss Publishers, 2008.

[24] E. Dionysian *et al.*, "Determination of joint stiffness of the human proximal interphalangeal joints: Development and clinical evaluation of a new device," in *Proceedings of the Annual International Conference of the IEEE Engineering in Medicine and Biology Society (EMBC)*, vol. 4, pp. 1546–1547, October-November 1992.

[25] E. Dionysian *et al.*, "Proximal interphalangeal joint stiffness: Measurement and analysis," *The Journal of Hand Surgery*, vol. 30, no. 3, pp. 573–579, 2005.

[26] D. J. Giurintano *et al.*, "A virtual five-link model of the thumb," *Medical Engineering and Physics*, vol. 17, no. 4, pp. 297–303, 1995.

[27] J. Lin *et al.*, "Modeling the constraints of human hand motion," in *Proceedings of Workshop on Human Motion (HUMO)*, Austin, USA, pp. 121–126, 2000.

[28] J. N. Goubier *et al.*, "Normal range-of-motion of trapeziometacarpal joint," *Chirurgie de la Main*, vol. 28, no. 5, pp. 297–300, 2009.

[29] M. R. Villareal, "Main division on the human hand." `http://commons.wikimedia.org/wiki/File:Scheme_human_hand_bones-en.svg`.

[30] V. Duindam, *Port-based modeling and control for efficient bipedal walking robots*. PhD thesis, University of Twente, The Netherlands, 2006.

[31] J. Pons *et al.*, "The MANUS-HAND dextrous robotics upper limb prosthesis: Mechanical and manipulation aspects," *Autonomous Robots*, vol. 16, no. 2, pp. 143–163, 2004.